Conference materials
UDC 538.911
DOI: https://doi.org/10.18721/JPM.161.115

Dimensional effect of nanocrystalline elements of the polyethylene structure

A.K. Borisov [1]✉, V.M. Egorov [1], V.A. Marikhin [1], L.P. Myasnikova [1]

[1] Ioffe Institute, St. Petersburg, Russia

✉ borisov.ak@mail.ioffe.ru

Abstract. The method for calculating the size distribution of nanocrystalline elements in lamellar and fibrillar polymer morphologies was proposed. The distribution of the longitudinal size of these elements in lamellas and microfibrils of ultrahigh molecular weight polyethylene was calculated using differential scanning calorimetry data. The calculation results are consistent with the data obtained by the X-ray method.

Keywords: ultrahigh molecular weight polyethylene, lamella, fibril, differential scanning calorimetry, phase transition

Citation: Borisov A.K., Egorov V.M., Marikhin V.A., Myasnikova L.P., Dimensional effect of nanocrystalline elements of the polyethylene structure, St. Petersburg State Polytechnical University Journal. Physics and Mathematics. 16 (1.1) (2023) 90–96. DOI: https://doi.org/10.18721/JPM.161.115

Материалы конференции
УДК 538.911
DOI: https://doi.org/10.18721/JPM.161.115

Размерный эффект нанокристаллических элементов структуры полиэтилена

А.К. Борисов [1]✉, В.М. Егоров [1], В.А. Марихин [1], Л.П. Мясникова [1]

[1] Физико-технический институт им. А.Ф. Иоффе РАН, Санкт-Петербург, Россия

✉ borisov.ak@mail.ioffe.ru

Аннотация. Предложен метод расчета распределения по размерам нанокристаллических элементов ламеллярной и фибриллярной надмолекулярных структур полимера. Расчет распределения продольного размера этих элементов в ламелях и микрофибриллах сверхвысокомолекулярного полиэтилена выполнен с использованием данных дифференциальной сканирующей калориметрии. Результаты расчетов согласуются с данными, полученными рентгеновским методом.

Ключевые слова: сверхвысокомолекулярный полиэтилен, ламель, фибрилла, дифференциальная сканирующая калориметрия, фазовый переход

Ссылка при цитировании: Борисов А.К., Егоров В.М., Марихин В.А., Мясникова Л.П., Размерный эффект нанокристаллических элементов структуры полиэтилена // Научно-технические ведомости СПбГПУ. Физико-математические науки. 2023. Т. 16. № 1.1. С. 90–96. DOI: https://doi.org/10.18721/JPM.161.115

Introduction

In the last decade, significant progress has been made in the creation of structural materials used in products that require high mechanical characteristics and special reliability. These materials include highly oriented fibers and threads obtained by gel technology from ultra-high molecular weight polyethylene (UHMWPE). They demonstrate high values of strength and elastic modulus [1, 2], but also have significant potential for their further increase, since the values currently obtained are significantly lower than theoretical estimates [3].

Since there is a relationship between the mechanical properties of polymeric materials and morphology, it is necessary to find out how the morphology is formed at each stage of fiber production. In this work, we propose a method based on the analysis of the shape of differential scanning calorimetry (DSC) melting curves, which makes it possible to obtain the size distribution of nanocrystalline elements in a polymer with various morphologies, including lamellar and fibrillar structures.

Samples and experiment

The thermophysical characteristics of the following samples were studied: the initial xerogel film obtained from a 1% solution in mineral oil of UHMWPE nascent powder with an average viscosity molecular weight $M_w = 3 \cdot 10^6$, and threads with different degrees of drawing obtained by multistage zone orientational hardening of the initial film on local heaters [4]. The samples listed above were studied using a DSC PerkinElmer calorimeter.

Figure 1 shows DSC curves that demonstrate the change in the melting peak of UHMWPE threads with increasing draw ratio (λ). It can be seen that the temperature of the maximum of the endothermic melting peak T_{max} shifts to high temperatures with increasing λ.

The shape of the peak also changes significantly: the amplitude increases, and at the first stage (λ < 50) a low-temperature shoulder is observed. At higher degrees of draw ratio the shoulder disappears, and the melting enthalpy ΔH and, accordingly, the degree of crystallinity increase by 10–30%. It is clear that the changes in the quantitative characteristics of the melting peak reflect the radical rearrangement of morphology that occurs in the polymer upon orientation. First, this affects crystalline formations, the melting point of which is different within a wide melting temperature range. Apparently, these crystalline formations differ from each other in size, since the same methylene groups $-CH_2-$ form them and, therefore, from the point of view of the internal structure, they are identical. In this case, the temperature interval and the shape of the endothermic melting peak are related to the size distribution of crystalline formations.

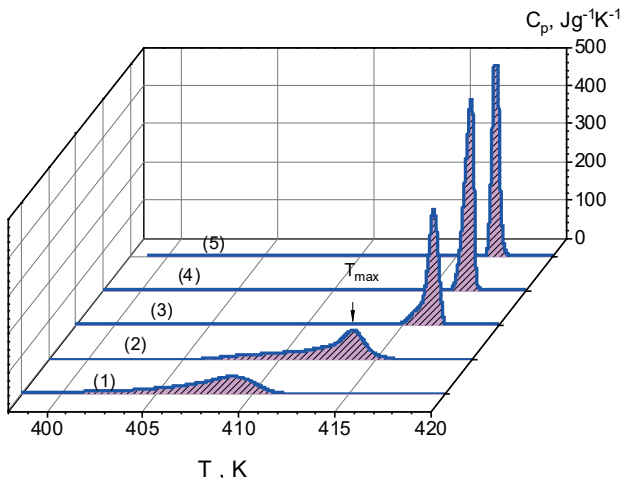

Fig. 1. DSC curves obtained by heating UHMWPE samples (V = 5 K/min). Initial film (1), oriented UHMWPE filaments with draw ratio λ = 9 (2), λ = 43 (3), λ = 95 (4), λ = 170 (5)

Theoretical calculations

Before calculating the distribution according to the experimental DSC curves shown in Figure 1, it is necessary to take into account the methodological error. In [5] we presented a method for determining the methodological error ΔT, according to which, under the same experimental conditions, the value of ΔT can be determined for one of the samples and used for the entire sample. In accordance with [6], extrapolation of the experimental linear dependence $T_{max} = f(V^{1/2})$ to $V = 0$ makes it possible to determine ΔT, which in our case was $\Delta T = 1.6$ K.

In [7] we proposed a method that makes it possible to obtain the size distribution of crystalline formations in a polymer by analyzing the shape of DSC curves. The method is based on the fact that during melting the heat flux is directly proportional to the mass fraction of crystallites that melt at temperature depending on their size. Therefore, the heat flux depending on the temperature can be converted into a heat flux distribution depending on the longitudinal size of the crystallite according to the following relation:

$$\mathrm{d}H / \mathrm{d}l_1 = \left(\mathrm{d}T / \mathrm{d}l_1\right)\left(\mathrm{d}H / \mathrm{d}T\right), \tag{1}$$

where $\mathrm{d}H/\mathrm{d}T$ is the experimental dependence of the heat flux on temperature, determined from the DSC curve, taking into account the scanning speed; l_1 is the longitudinal size of the crystallite, equal to $l_1 = h \times n$, where n is the number of C-C bonds in the main chain, h is the length of the bond projection onto the axis of the macromolecule (for polyethylene, $h = 0.124$ nm). The dependence $\mathrm{d}T/\mathrm{d}l_1$ is obtained from the generalized Gibbs Thomson equation based on the balance of surface and volume energies [8, 9]:

$$T(l_1) = T_0[1 - 2 / \Delta H_0(\sigma / l_2 + \sigma / l_3 + \sigma_e / l_1)], \tag{2}$$

where l_2 and l_3 are the dimensions of the crystallite in the plane perpendicular to the longitudinal axis of the macromolecule; σ is the surface energy of the side surfaces of the crystallite; σ_e is the surface energy of the end surface; $\Delta H_0 = 293$ J/cm^{-3} and $T_0 = 415$ K are the enthalpy of phase transition and the melting point of an ideal polyethylene crystal [6], respectively.

In the initial xerogel film the UHMWPE morphology consists of stacks of lamellae; l_2 and $l_3 >> l_1$. Therefore, in expression (2) the terms σ/l_2 and σ/l_3 can be neglected:

$$T\left(l_1\right) = T_0[\,1 - 2\,\sigma_e / \Delta H_0 l_1)] \tag{3}$$

However, the distribution $\mathrm{d}H/\mathrm{d}l_1$ calculated from relations (1) and (3) is not a distribution of the number of lamellas versus thickness, since thicker lamellas absorb more heat. This distribution cannot be compared with distributions obtained by other methods that determine the number of lamellae of a certain thickness. Therefore, for a correct comparison, it is necessary to normalize to l_1. Figure 2 (curve 1) shows the calculation of $l_1^{-1} \cdot \mathrm{d}H/\mathrm{d}l_1$ as a percentage for the initial non-oriented sample. The calculations used the value of the surface energy $\sigma_e = 9 \cdot 10^{-6}$ J/cm^2 [8]. It can be seen from the figure that the maximum number of lamellae is in the range of 6–8 nm (18%), and the bulk of lamellae (~ 80%) have thicknesses from 4 to 14 nm.

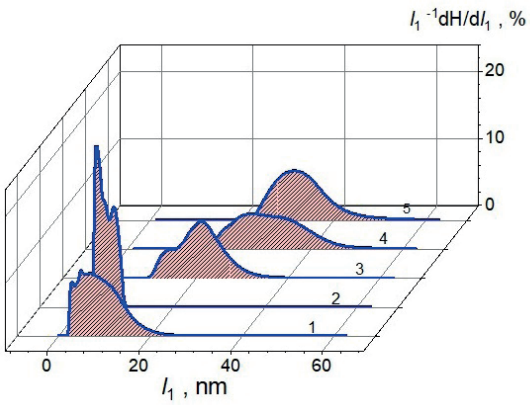

Fig. 2. The dependence of the number of crystalline formations on their longitudinal size, expressed as a percentage. Initial film (1), oriented UHMWPE with draw ratio $\lambda = 9$ (2), $\lambda = 43$ (3), $\lambda = 95$ (4), $\lambda = 170$ (5)

The lamellar morphology of the initial xerogel film undergoes strong changes during orientational drawing: the lamellar structure is rearranged into a fibrillar one [1]. It is known [3] that the morphology of a fibril consists of a successive alternation of crystalline and disordered regions, in which a large number of macromolecules emerging from the previous crystallite pass into the next one. The parameters l_2 and l_3 of the crystalline regions of fibrils are comparable with l_1. In the first approximation, the surface energy can be considered the same for all side surfaces and, therefore, only the end σ_e and lateral σ surface energies can be used. Thus, the dimensions of the cross section of crystallites will be equal: $l_2 = l_3 = l$. Expression (2) takes the following form:

$$T(l_1) = T_0[\,1 - 2 / \Delta H_0 (2\sigma / l + \sigma_e / l_1)] \tag{4}$$

To determine the surface energy σ, i.e., energy of intermolecular interaction per unit area ~ 0.2 nm^2 of the methylene group $-CH_2-$, it is necessary to determine the part of the cohesive energy E_c = 3.6 kJ/mol [10], which is related to the van der Waals interaction in the disordered phase. It is known [10] that this part is (0.35 ± 0.05) E_c. An estimate based on the above parameters gives the value of the lateral surface energy equal to $\sigma \approx 9$ erg/cm^2.

The value of the end surface energy σ_e associated with intrafibrillar disordered regions is much more difficult to determine. It is worth noting here that it is the structure of these regions that controls the orientational strength of the oriented polymer. There are several models [11] that describe the structural elements of intrafibrillar disordered regions. Figure 3 schematically shows the most significant of them. To obtain a complete understanding of the formation of the end surface of crystallites, a detailed analysis of these elements is required.

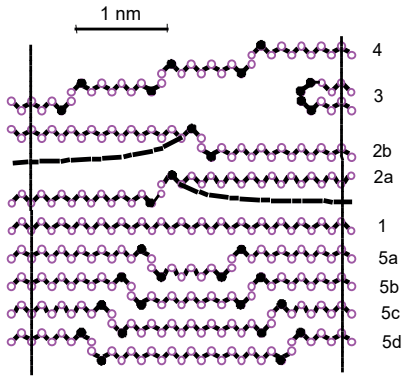

Fig. 3. Structural elements of the intrafibrillar region of the microfibril. Dashed lines are the boundaries of crystalline formations. Filled circles are gauche isomers

Let us consider the possibility of occurrence of the elements shown in Figure 3:

1 – crystalline bridges or completely straightened molecules in the trans-conformation between adjacent microfibril crystallites (see Fig. 3, position 1). The presence of such structures is confirmed by X-ray studies [12], which found that the effective average crystallite size exceeds a large period, which can be explained by a significant number of straightened molecules in the disordered regions of microfibrils;

2 – conformational defects in straightened segments of macromolecules formed by a *kink* isomer, consisting of a combination of the simplest isomers with *trans* and *gauche* conformations. Low energy *trans* conformations are denoted by *t* and higher energy conformations by *g*. Thus, the simplest *kink* conformer with *ttt-g-t-g-ttt* alternation is denoted by 2*g*1. According to the so-called crankshaft model [8], kink isomers are represented as differently directed steps on a macromolecule (see Figure 3, positions 2, *a*, *b*). The 2*g*1 conformers are equilibrium defects. According to an alternative model [12], a conformational defect in a straightened segment of a macromolecule is a step with a small segment of the chain adjusting as it moves away from the turning point of the chain (see Fig. 3, positions 2, *a*, *b*, dash-dotted lines);

3 – irregular and regular loops formed by returning some of the molecules to the same crystallite from which they left. Four *gauche* conformers form regular loops or folds that form the surface of the crystals in the lamellae (see Fig. 3, position 3). More *gauche* conformers form irregular loops;

4 – curved tie molecules connecting the crystallites to each other (see Fig. 3, position 4). Curvature due to the presence of one *gauche* isomer on each side of neighboring crystallites. The degree of curvature is determined by the number of *gauche* isomers that can lie in between these "surface" *gauche* isomers;

5 – the "crankshaft" structure formed by multidirectional steps or *kink* isomers [14] (see Fig. 3, position 5, *a*). The possibility of the existence of a combination of such structures is assumed (see Fig. 4, positions 5, *b*, *c*, *d*). It is based on the fact that if the excess volume of one step is $3/4v_0$, where v_0 is the volume of the CH_2 group, then the excess volume of each of the contributing steps is only $1/4v_0$ [15], i.e., in this case, a cooperative effect is observed.

The orientational drawing of the polymer occurs at elevated temperatures and is accompanied by an increase in the degree of crystallinity. It is carried out by reducing the defectiveness of the disordered interlayer. The molecular mechanism of this process is associated with multidirectional diffusion of *kinks* or *double kinks* along the polymer chain, followed by annihilation at the ends of macromolecules or the formation of a crankshaft type defect and their combinations.

Each of the above combinations of isomers in the intrafibrillar region makes a different contribution to the end surface energy. For *kink* defects (see Fig. 3, positions 2 and 2*a*) containing two *gauche* isomers, the surface energy is determined by one gauche isomer, since the step forms the elementary surface of two adjacent crystals. In the case of the "crankshaft" (see Fig. 3, positions 5*a*, *b*, *c*, *d*), the surface energy is produced by two *gauche* isomers, and finally in the case of a regular fold (see Fig. 3, position 3), by four. Curved tie molecules that connect the crystallites to each other (see Fig. 3, position 4) are straightened due to the diffusion of *kinks* during orientational drawing at elevated temperatures and then turn into steps (see Fig. 3, positions 2 and 2, *a*).

To determine the end surface energy σ_e created by one gauche isomer, it is necessary to find the fraction of the formation energy of this defect $\Delta E = 2.5$ kJ/mol per unit area $\Delta S \approx 0.18$ nm^2 of the chain end surface. An estimate of the ratio $\Delta E/\Delta S$ gives the value of the end surface energy equal to $\sigma_{e1} \approx 11$ erg/cm^2. In the case of the "crankshaft", the surface energy already formed by two *gauche* isomers will be twice as high ($\sigma_{e2} \approx 22$ erg/cm^2).

To calculate dH/dL using relations (1) and (4) for a fibrillar structure, in addition to the values of the end and side surface energies, it is necessary to determine the parameter l, the size of the microfibril in cross section. Figure 2 (curves 2–5) shows the calculation of the dH/dL distribution for oriented PE samples with fibrillar morphology. In calculations $l = 40$ nm and $\sigma_{e1} \approx 11$ erg/cm^2 were used.

Figure 2 shows the complex nature of the change in the size distribution of crystallites with orientation. At the first stage of orientation (curve 2) a sharp decrease in the width of the distribution and a shift to low dimensions are observed. This is due to the transition from the lamellar morphology of the original sample to the fibrillar one with a large proportion of the disordered part. Further orientation is accompanied by an increase in the size of crystalline regions, an increase in the spreading of distributions, and a decrease in the proportion of the disordered part (see Fig. 2, curves 3–5).

To compare the obtained distributions with the X-ray data published in [12], it was necessary to determine the weighted average lm in the dH/dl_1 distribution. The value of l_m was determined by the relation $l_m = \Sigma\, l_i(dH/dl_1)_i/\Sigma\, (dH/dl_1)_i$, where l_i is the current value of l_1 in the distribution; $(dH/dl_1)_i$ is the current value of dH/dl_1 at $l_1 = l_i$.

Figure 4 shows the dependences of the weighted average values of the longitudinal sizes of crystallites l_m on the degree of orientation of the initial xerogel film, obtained from X-ray data (1) and calculated values of l_m (2, 3). It can be seen from the figure that the distributions of the longitudinal sizes of crystallites obtained on the basis of X-ray (1) and DSC data (2) fit into one dependence. In this case, the value of the end surface energy σ_{e1} created by one gauche isomer was used in the calculations.

It can be seen from the figure that the dependence sharply increases at the initial stage, and then, in the range $\lambda \approx 50$–150, it reaches saturation. This process is associated with the diffusion of kinks or double kinks that form the surface energy σ_{e1}, since they either annihilate upon reaching the end of the chain or meet with a double kink in the opposite direction and form a "rankshaft" structure. With a large number of these elements in the limited space of the intrafibrillar region, they can cooperate into a structure similar to that shown in Figure 3 (positions 5*a*, *b*, *c* and *d*).

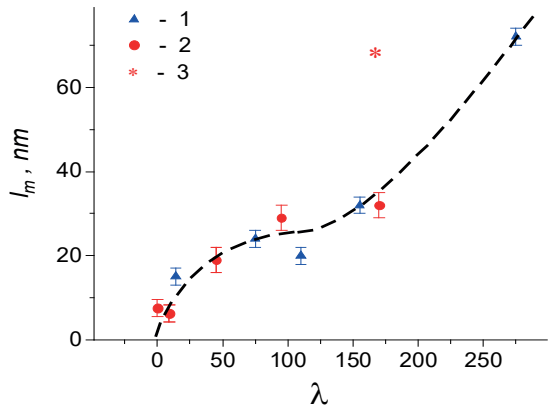

Fig. 4. Dependences of the weighted average values of the longitudinal sizes of crystallites on the degree of orientation according to X-ray data (1) and calculated at σ_{e1} (2) and σ_{e2} (3).

In such a structure, the cooperative excess volume will be less than the sum of the excess volumes of the independent elements of this structure.

For ultra-high orientation draw ratio ($\lambda \approx 270$) there is a sharp increase in $l_m(\lambda)$ (see Fig. 4). According to relation (4), such a rise can be caused by two reasons. First, the inclusion of crystalline formations with increased end surface energy into the process of orientational ordering. The calculation using the value of the end surface energy σ_{e2}, formed by the elements of the crankshaft type structure, indeed shows (see Fig. 4, position 3) a significant increase in l_m. An increase in the drawing temperature, which can exceed the melting temperature of an equilibrium PE crystal [16], leads to an acceleration of diffusion and annihilation of complex combinations of defects on the surface of crystalline formations, which leads to a high surface end energy.

The second reason for the sharp rise may be the dependence of l_m on the transverse size of the crystallite, i.e., on the parameter l in relation (4). Such a process should occur as the density of defects in the disordered interlayer decreases and the number of crystalline bridges in the *trans* conformation between neighboring crystallites in the microfibril increases. In the limiting case (at $l_m \to \infty$), relation (4) implies that the parameter l tends to 0.1–0.2 nm, i.e., the transverse size of the crystallite becomes comparable to the transverse size of a single polyethylene chain.

Conclusion

Thus, the method proposed in this work for calculating the size distribution of nanocrystalline elements of lamellar and fibrillar polymer morphologies made it possible to reveal a number of features of the process of orientational drawing of ultrahigh molecular weight polyethylene. Based on the analysis of these features, a model is proposed that describes the evolution of the disordered part of the polymer morphology. The results of calculations based on the weighted averages in the distribution obtained from calorimetric data are consistent with the data obtained by the X-ray method.

REFERENCES

1. **Marikhin V., Myasnikova L., Boiko Yu., Ivan'kova E., Radovanova E., Yakushev P.,** Reactor Powder Morphology, Ch. 10, Nova Publishers. New York (2011).

2. **Boiko Y.M., Marikhin V.A., Moskalyuk O.A., Myasnikova L.P.,** On the determination of the elastic modulus of ultraoriented high-strength film threads obtained by drawing of ultra-high-molecular-weight polyethylene xerogels, Physics of the Solid State. 61 (44) (2019) 44–47.

3. **Marikhin V.A., Myasnikova L.P.,** Structural basis of high-strength high-modulus polymers, Oriented Polymer Materials. (1996) 38–98.

4. **Marikhin V.A., Myasnikova L.P.,** Heterogeneity of structure and mechanical properties of polymers, Makromol. Chemie. Macromol. Symp. B. 41 (1991) 209–227.

5. **Egorov V.M., Borisov A.K., Marikhin V.A.,** Formation of nanonuclei during a structural phase transition in molecular crystals of normal alkanes, Physics of the Solid State. 63 (3) (2021) 498–504.

6. **Illers K.-H.,** Die ermittlung des schmelzpunktes von kristallinen polymeren mittels wärmeflusskalorimetrie (DSC), European Polymer Journal. 10 (10) (1974) 911–916.
7. **Egorov V.M., Borisov A.K., Marikhin V.A.,** Thermal conductivity of a composite based on n-alkane and nanosized additives, Technical Physics Letters. 48 (1) (2022) 49–52.
8. **Wunderlich B.,** Macromolecular physics, Vol. 3. Academic Press. London (1980).
9. **Hoffman J.D.,** Treatise on solid state chemistry, Vol. 3. Plenum Press. New York (1976).
10. **Van Krevelen D.W.,** Properties of polymers correlations with chemical structure. New York (1972).
11. **Marikhin V.A., Myasnikova L.P.,** Nadmolekulyarnaya struktura polimerov, Chemistry. Leningrad (1977).
12. **Marikhin V.A., Myasnikova L.P., Uspensky M.D.,** Features of orientation drawing of gel-crystallized polyethylene, Polymer Science Series A. 35 (6) (1993) 686–692.
13. **Gotlib Y.A., Darinskiy A.A., Svetlov Y.E.,** Fizicheskaya kinetika makromolekul, Chemistry. Leningrad (1986).
14. **Marikhin V.A.,** The structure of amorphous sections of microfibrils of oriented polymers, Physics of the Solid State. 19 (4) (1977) 1036–1039.
15. **Kausch H.,** Polymer fracture, Plenum Press. Springer-Verlag, Berlin (1978).
16. **Bershtein V.A., Savitsky A.V., Egorov V.M.,** Melting of polyethylene with strength close to theoretical, Polymer Science Series A. 27 (2) (1985) 113–116.

THE AUTHORS

BORISOV Artem K.
borisov.ak@mail.ioffe.ru
ORCID: 0000-0001-8010-5467

EGOROV Victor M.
victor_egorov1@inbox.ru
ORCID: 0000-0002-8742-2710

MARIKHIN Vyacheslav A.
v.marikhin@mail.ioffe.ru
ORCID: 0000-0001-7088-5914

MYASNIKOVA Lyubov P.
liu2000@mail.ru
ORCID: 0000-0003-0648-5056

Received 19.10.2022. Approved after reviewing 14.11.2022. Accepted 15.11.2022.